Available online at www.sciencedirect.com
SCIENCE DIRECT®
Journal of Magnetic Resonance 163 (2003) 270–276
JMR Journal of Magnetic Resonance
www.elsevier.com/locate/jmr

The effect of relaxation on the epitope mapping by saturation transfer difference NMR

Jiangli Yan, Allen D. Kline, Huaping Mo, Michael J. Shapiro,* and Edward R. Zartler

Discovery Chemistry Research and Technologies, Lilly Research Labs, Lilly Corporate Center, Eli Lilly & Co, Indianapolis, IN 46285, USA

Received 27 December 2002; revised 5 March 2003

Abstract

The effect of longitudinal relaxation of ligand protons on saturation transfer difference (STD) was investigated by using a known binding system, dihydrofolate reductase and trimethoprim. The results indicate that T1 relaxation of ligand protons has a severe interference on the epitope map derived from a STD measurement. When the T1s of individual ligand protons are distinctly different, STD experiments may not give an accurate epitope map for the ligand–target interactions. Measuring the relaxation times prior to mapping is strongly advised. A saturation time shorter than T1s is suggested for improving the potential epitope map. Reduction in temperature was seen to enhance the saturation efficiency in small to medium size targets.

Keywords: Epitope mapping; Saturation transfer difference (STD); Effect of T1 relaxation

1. Introduction

In biochemical and pharmaceutical research, identification of the binding activity and characterization of the binding epitope of ligands is important to lead validation and optimization in drug discovery. Many NMR-based methods have been developed for detecting the binding interactions between small ligands and biomolecular targets. Target-based methods rely on the perturbations of $^{1}H/^{15}N/^{13}C$ chemical shifts due to ligand binding and can be utilized to map the binding site on the protein target [1–3]. By directly detecting the ligand signals, several different methodologies have been developed to determine binding affinities of potential candidates. These ligand-based techniques include transferred NOE [4–8], inter-ligand NOE [9–11], diffusion [12–14], relaxation [15–17], NOE-pumping [18,19], ligand release [20,21], waterLOGSY [22,23], and saturation transfer difference [24–26]. Although NMR-based techniques are not as sensitive as other commonly used methods in high-throughput drug screening, such as mass spectrometry, NMR has been considered comparatively robust in drug discovery since it is less prone to give artifacts [21]. In addition, NMR is able to supply more detailed structural information, such as the binding epitope for both target and ligand using target-based and ligand-based methods, respectively.

Saturation transfer difference (STD) is a fast and versatile method for screening binding components from a mixture [25,26]. It is based on magnetization transfer by protein signal saturation and its relayed effect to ligand. Macromolecules have a large network of protons that are tightly coupled by dipole–dipole interactions. Saturation of a single protein resonance can result in a rapid spread of the saturation over the entire protein if spin diffusion within the protein is efficient. During the saturation period, progressive saturation transfers from the protein to the ligand protons if the ligand binds to the target. The ligand protons nearest to the protein should be saturated to the highest degree and therefore, have the strongest signal in the STD spectrum. The ligand protons, which are further from the target surface will be saturated to lower degree and their STD intensities will be weaker. Therefore, the degree of saturation of individual ligand protons reflect their proximities to the protein surface and can be used as an epitope method to describe the target–ligand interactions

* Corresponding author.
E-mail address: shapiro_michael@lilly.com (M.J. Shapiro).

1090-7807/$ - see front matter © 2003 Elsevier Science (USA). All rights reserved.
doi:10.1016/S1090-7807(03)00106-X

[7,27–29]. Here we present a study of STD epitope mapping using a well-known system, dihydrofolate reductase (DHFR) and trimethoprim (TMP) [30–36]. It is found that the STD epitope values are greatly affected by longitudinal relaxation. When the longitudinal relaxation time of individual protons are significantly different, the resulting STD does not produce an accurate epitope map for the ligand–target interaction.

2. Methods

One times phosphate-buffered saline (PBS) of D_2O containing 10 mM sodium phosphate, 0.16 M NaCl, and 3 μM NaN_3 at pH 7.3 was used to prepare all the NMR samples. Dihydrofolate reductase (EC 1.5.1.3) from bovine liver and trimethoprim were purchased from Sigma. Prior to use, DHFR was dialyzed extensively and TMP was dissolved into PBS buffer. 4.2 mM of TMP, 4.2 mM of TMP with 120 μM DHFR, and 100 μM DHFR solutions were prepared to test the ligand–target binding.

All NMR experiments were performed on Bruker Avance DRX 600-MHz and 500-MHz spectrometers using 5-mm inverse triple-resonance ($^{15}N/^{13}C/^{1}H$) probes equipped with triple axis actively shielded gradients. STD [27] spectra were collected with 16 k data points to cover a sweep width of 12 ppm. Selective saturation of the protein was performed using a Gaussian pulse train. The shaped pulse with a length of 8.5 ms was followed by a short delay of 4 ms and the total saturation time was adjusted by the number of pulses in the train. The intensity of the Gaussian pulse corresponded to a strength of 59 Hz. An additional delay before saturation was applied to keep the total recovery time constant. The saturated and reference spectra were acquired and processed simultaneously by creating a pseudo-2D experiment. The saturation frequency switched from on-resonance (for instance, 0.9 ppm) for the saturated spectrum to off-resonance (usually −10 ppm) for the reference after each scan. A CPMG [37,38] T2-filter with a total length of 32.4 ms was used to eliminate protein background signals. W3 WATERGATE [39] pulse train was used to suppress the H_2O signal. The spectra were processed using Bruker Xwinnmr. A cosine^2 function prior to zero-filling by a factor of 2 was applied before Fourier transform. STD spectrum was obtained by subtraction of saturated spectrum from the reference spectrum and STD intensity of individual signal was measured relative to the corresponding signal intensity in the reference spectrum.

Longitudinal relaxation time T1 of the ligand TMP was measured when the protein DHFR was present. The standard inversion recovery method was used for the measurements with a relaxation delay of 15 s. Data points (16 k) were acquired to cover a sweep width of 10 ppm. A cosine^2 function and a zero-filling by a factor of 2 was applied before Fourier transfer. Data were analyzed using Bruker Xwinnmr.

3. Results

In principle, the saturation degree of an individual ligand proton reflects the proximity of this proton to the target surface. When creating an epitope map, the STD intensity relative to the reference is used to create the binding epitope maps, this is usually described by the STD factor A_{STD}, as shown by Eq. (1):

$$A_{std} = \frac{I_0 - I_{sat}}{I_0} = \frac{I_{STD}}{I_0}. \quad (1)$$

If different systems are compared, ligand excess should be used to normalize the differences of protein concentration [27]. Fig. 1 presents the STD spectrum and epitope map of 4.2 mM of TMP in the presence of 120 μM DHFR (with a molar ratio of ligand to protein of 35). The data shown on the spectrum are STD intensities relative to the reference (Eq. (1)). A saturation time of 2.0 s was used. It was verified by DHFR only that 2.0 s was sufficient to saturate all the site of DHFR. The STD epitope map of TMP binding to DHFR (numbers on the structure) was obtained by normalizing the largest value to 100.

A build-up curve of STD factor A_{std} against the saturation time was used to study the time course of STD epitope mapping [25,27]. Fig. 2 shows the build-up

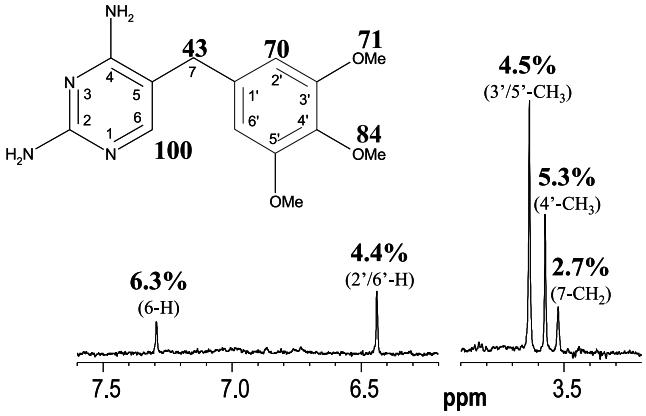

Fig. 1. STD spectrum of 4.2 mM TMP in the presence of 120 μM DHFR recorded at 298 K on a 600 MHz spectrometer. STD intensities relative to the corresponding reference intensities are shown on each signals with bold percentage numbers, the assignment of each signal is indicated in the bracket under STD intensity. The bold numbers on the structure are the STD epitope map by normalizing the largest STD intensity to 100. The small numbers on the structure are atom ID. The pre-saturation time of STD experiment was 2.0 s with a total recovery delay of 4.0 s. DHFR was irradiated with a Gaussian shaped pulse train at 0.9 ppm. A CPMG T2 filter of 32.9 ms was used to eliminate the protein background. The reference spectrum was recorded by irradiating at −9.5 ppm.

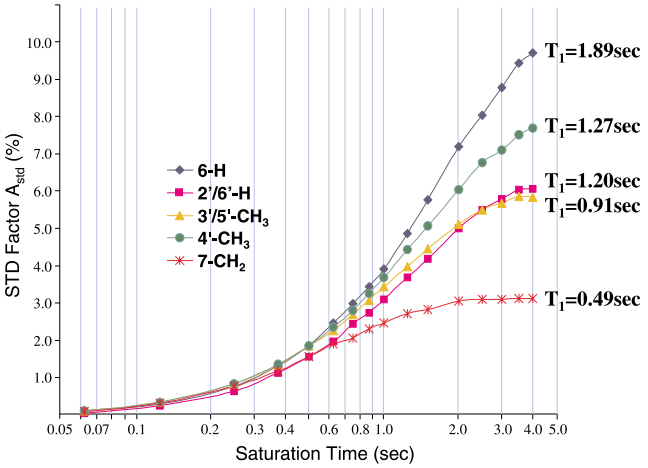

Fig. 2. Plot of STD factor of TMP–DHFR system via the saturation time in the log scale. STD experiments were performed at 298 K on a 600 MHz spectrometer. The protein was irradiated with a Gaussian shaped pulse train at 0.9 ppm for saturated spectrum and at −9.5 ppm for reference spectrum. The total recovery delay was set to 4 s and the presaturation time was adjusted by the number of shaped pulses in the train. A CPMG T2 filter of 32.9 ms was used. T1 relaxation time of each signals measured at the same temperature in the presence of DHFR are also presented.

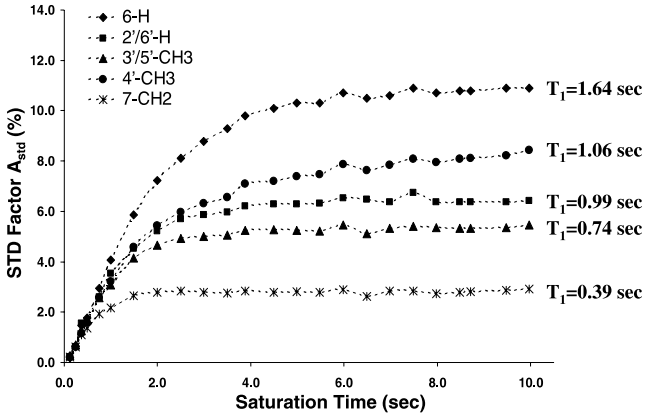

Fig. 3. Plot of STD factor of TMP binding on DHFR against the saturation time. STD experiments were performed at 277 K on a 500 MHz spectrometer. The protein was irradiated with a Gaussian shaped pulse train at 0.9 ppm for saturated spectrum and at −9.5 ppm for reference spectrum. The total recovery delay was set to 10 s and the presaturation time was adjusted by the number of shaped pulses in the train. A CPMG T2 filter of 32.9 ms was used. Longitudinal relaxation time of each signals measured in the presence of DHFR are also presented.

curves for TMP–DHFR system in the log scale of x-axis. The exchange-averaged T1 values of TMP, measured when protein DHFR was present, are also shown. When DHFR is saturated less than 250 ms, the methylene protons with a T1 of only 0.49 s (red stars) have strong STD, but the STD build-up slows and reaches the plateau before the protein has been irradiated for 2 s. The T1 of 6-H (blue diamonds) is the longest, and it has the longest time to build-up until it plateaus. The STD intensity of 2′/6′-H signal (pink squares) is weak when the saturation time is shorter than 0.5 s. Because its T1 is relatively long (1.2 s), its STD keeps rapidly building up until the saturation time increases to 3.5 s at which point it plateaus. These results indicate that T1 has a strong effect on the rates of STD build-up. Fig. 2 also presents that different saturation time yields different pattern of epitope map for TMP–DHFR system. For example, the epitope value of 2′/6′-H is the smallest when the saturation time is shorter than 0.4 s, then is the second smallest between 0.4 and 2.5 s, and then is the third smallest after DHFR is irradiated for 2.5 s. If the saturation time is shorter than 0.25 s, the methylene signal has third largest A_{STD}. When the protein was saturated for 0.25 s, the order of A_{STD} is 4′-CH3 and 3′/5′-CH3 (0.87 for both), 7-CH_2 (0.85), 6-H (0.79) and 2′/6′-H (0.66). The A_{STD} of 7-CH_2 ranks in the second smallest when the saturation time is longer than 0.25 s but shorter than 0.50 s where it drops to the smallest.

Fig. 3 is another plot of A_{STD} against saturation time with the saturation time up to 5 times of T1. Data were collected at 277 K and the corresponding exchange-averaged T1's are shown in Fig. 3. The data indicates that a very long saturation does not help increasing the STD sensitivity and a very short saturation time is not favorable either due to the low signal intensity of STD. Typically, a saturation time of 1–2 s is used in STD experiments [24,28,29]. STD intensities build-up rapidly first when the saturation time is increased, from 0 to 4 s for 6-H for example. Then the build-up slows and the STD intensity reaches a plateau after a certain period of saturation. The STD curve for a given proton can be defined by two regions: the build-up region and the plateau region. Therefore, the STD build-up can be described by the build-up rate (for the first part of the curve) and the relative height of the plateau (for the other part of the curve). The average value of $\bar{A}_{STD}$ on the plateaus, $\bar{A}_{std}$, is used to define the STD plateau height. The $\bar{A}_{std}$ value of each signal was derived from those points in Fig. 3 with a saturation time longer than its 5 times of T1 and are shown in Table 1. The shortest saturation time τ_p for each signal to reach the plateau is also listed in Table 1. τ_p was obtained from the first point (with the shortest saturation time) to have an $\bar{A}_{std}$ of $(1 \pm 5\%) \times \bar{A}_{std}$. τ_p and $\bar{A}_{std}$ describe the relative rate of STD build-up and the relative height of the plateau, respectively, and therefore, represent the total STD build-up curve shown in Fig. 3. It can be seen from Table 1 and Fig. 3 that the order of STD build-up time τ_p is the order of T1 relaxation time. The shorter the T1 relaxation time, the earlier the STD plateaus. The signal of 6-H has the longest T1 and therefore, has the longest τ_p or the slowest rate of STD build-up. The similarity of the normalized (to the smallest) T1 and $\bar{A}_{std}$ of each

Table 1
Comparison of the relative amplitudes of T1 relaxation time and average STD data obtained with saturation time from 5 times of T1 to 10 s of each signal

H signal	T1 relaxation		STD		
	T1 (sec)[a]	T1/T1(shortest)[b]	$\bar{A}_{std}$[c]	$\bar{A}_{std}/\bar{A}_{std(weakest)}$[d]	τ_p[e] (sec)
6-H	1.64	4.2	10.85	3.9	4.98
2′/6′-H	0.99	2.5	6.42	2.3	3.87
3′/5′-CH_3	0.74	1.9	5.32	1.9	3.49
4′-CH_3	1.06	2.7	7.24	2.6	3.87
7-CH_2	0.39	1.0	2.80	1.0	1.99

[a] T1 was measured in the presence of DHFR.
[b] T1(shortest) is the T1 value of 7-CH_2 shown in column 2, that is 0.39 s.
[c] $\bar{A}_{std}$ here represents the average A_{STD} obtained from the data shown in Fig. 3 with saturation time longer than 5 times of T1 of each signal.
[d] $\bar{A}_{std(weakest)}$ is the $\bar{A}_{std}$ value of 7-CH_2 shown in column 4, that is 2.80.
[e] τ_p is the shortest saturation time for the individual signal to have an A_{std} of $(1+5\%)\times\bar{A}_{std}$.

signal shows that STD plateau is also dominated by the corresponding T1 relaxation. The T1 ratio of 3′/5′-CH_3 to 7-CH_2 is 1.9 and their $\bar{A}_{std}$ ratio at plateau is approximately the same. 4′-CH_3's T1 is 2.7 times of the T1 of 7-CH_2 and its STD is 2.3 times stronger than 7-CH_2. Since both the build-up rate and the height of the plateau are strongly affected by T1 relaxation, the relative STD intensities or the STD epitope values are ordered in accordance by their T1 relaxation times after a certain period of saturation, 1.5 s in this specific case.

When TMP binds to DHFR ($K_a = 2\times10^7\ M^{-1}$) [30], the pyrimidine N1 is protonated and 1-NH and 2-NH_2 are involved in hydrogen bonds [31,40]. The X-ray structure shows that TMP binds in the active site of DHFR with its pyrimidine ring and C7 methylene being held in the interior of a deep cleft, while the trimethoxy-benzyl side chain extends out toward the entrance of the binding pocket [33,34]. In all 12 restrained minimized structures of DHFR-TMP reported by Feeney and coworkers [31], three amino acids have intermolecular H–H distances smaller than 3.5 Å to the H6 of TMP. There are two residues within 3.5 Å to one of the H7 protons, and parts of another residue are close to the other H7. The ring-flipping of the trimethoxy-benzyl ring of the TMP in the binary and ternary complexes of DHFR–TMP suggests a lack of consistent contact with DHFR at the trimethoxy-benzyl ring [40]. The early modification of TMP for receptor-based design of DHFR inhibitors [35,36] also yields the same results. According to the STD epitope mapping shown in Fig. 1, only the aromatic proton 6-H is close to DHFR while the methylene 7-CH_2 protons are not in intimate contact with DHFR. The evaluation at 7-CH_2 is contrary to the known binding model. The reason for this discrepancy is that the T1 relaxation time of 7-CH_2 protons is very short, only 0.49 s at 298 K.

During the saturation period, protein is saturated by a selective irradiation and progressive saturation transfers from the protein to the ligand protons. The transferred saturation is related to the intermolecular cross-relaxation or the intermolecular NOE. When the saturation time is short and if all sites of the protein are sufficiently saturated in this short period of saturation, A_{STD} reflects the proximity of the ligand protons to the protein surface. But when a long saturation time is used, competition occurs between intermolecular saturation-transfer and other procedures. The longitudinal T1 relaxation is a major one of them. If a long saturation time is used and all STD signals have reached their maximum, STD epitope mapping is totally controlled by T1 relaxation and is not accurate. For the study of binding, a short saturation time is recommended to minimize the effect of T1 relaxation on the epitope map. But it is difficult to quantitatively correlate the T1 relaxation rate and the intermolecular cross-relaxation rate since the relaxation of the ligand–target system during saturation is complicated. A too short saturation may also cause insufficient saturation of the entire protein. Although a

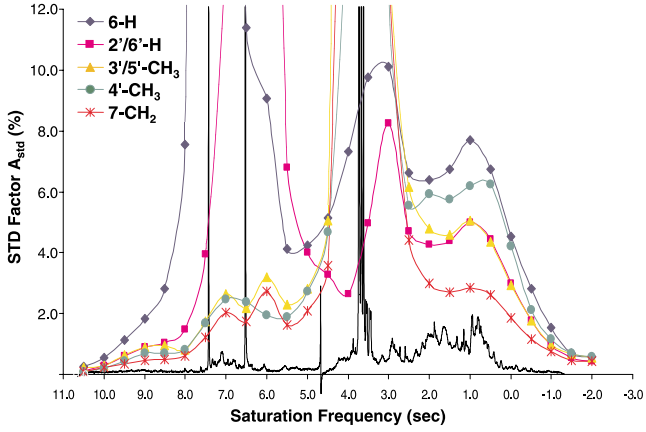

Fig. 4. Plot of STD factor via the saturation frequency (colored curves) and 1D ^{1}H spectrum (black curve) of 4.0 mM TMP with 120 μM DHFR. STD experiments were performed at 298 K on a 600 MHz spectrometer. The protein was irradiated with a Gaussian shaped pulse train for 2.0 s and an additional recovery time of 1.0 s was applied before saturation. A CPMG T2 filter of 32.9 ms was used. 1D ^{1}H spectrum was recorded with a relaxation delay of 2.0 s.

saturation period shorter than half of the shortest T1 is desired to eliminate the effect of relaxation, the sensitivity of STD under this condition is greatly reduced. When the saturation time was set to less than 250 ms (half of the shortest T1 of this system), less than 1% STD could be observed under optimal conditions for this system. It was also found that when the saturation time was short the methyl signals 4′-CH_3 and 3′/5′-CH_3 had strong STD indicating they are closest to the target. This does not agree with the previous NMR [30–32] and crystallography [33,34] studies. It may be caused by their strong signal intensities. It is easier to measure STD of strong methyls when other signals are close to the level of noise.

The problem of sensitivity will be more severe when short saturation is applied and the saturation frequency is far away from strong protein signals. Fig. 4 presents the plot of STD factor A_{STD} via the saturation frequency with the 1D ^{1}H spectrum of TMP with DHFR (black curve) overlapping. For TMP with five singlets between 7.4 and 3.5 ppm, the usable saturation frequency is limited to a narrow range of lower than 1.5 ppm and higher than 9.5 ppm. Otherwise the signal of TMP would be perturbed by the selective shaped pulse and extremely strong signals (that do not result from transferred saturation) would be observed in the difference spectrum. Within the usable range, STD builds up rapidly when strong protein signals are irradiated. Saturation on protein methyl signals around 0.9 ppm yields strongest saturation of ligand. Relative STD intensity drops to below 1% when DHFR is saturated out of the range of −1.0 to 1.5 ppm.

The saturation efficiency of the target is a key factor for improving the strength of STD signals of ligand. Beside saturation duration and offset, the correlation time of the target is another factor that affects the efficiency of saturation. It is found that lowering the temperature helps to enhance the transferred saturation. Shown in Fig. 5 is the temperature effect on the STD of TMP–DHFR system. A 2.5 times enhancement was observed when the temperature was changed from 303 to 277 K. Temperature may affect other factors relevant to STD intensity, such as dissociation-rate constant of binding and longitudinal relaxation rates of both ligand and target protons. It was found that as the temperature was lowered the STD intensity increased even though T1 decreased. We believe that the predominant factor for STD enhancement via reduction of temperature is the reduced molecular tumbling. The slow tumbling of protein accelerates the spread of saturation over the entire protein and the progressive transfer of saturation to the bound ligand. The bigger the protein, the easier it is to saturate the entire protein. Fig. 6 displays the saturation of DHFR at 277 (black) and 303 K (red) irradiated by shaped pulse for 2.0 (a) and 0.5 s (b). For comparison, the spectra were scaled to the overlapped (equal intensity) references. The protein was saturated on the methyls at 0.9 ppm. Although the signals near the saturation frequency have similar intensities, the signals elsewhere recorded at 277 K are much stronger than those recorded at 303 K. To saturate the entire protein (to get flat signals beyond the saturation frequency on the saturated spectrum), at 277 K only 1.5 s was used while 4.5 s had to be applied at 303 K. This effect is more important for the target of small size, at least for DHFR (22 kDa), when short saturation times have to be used (Fig. 6b). Significant increases were observed for other proteins with molecular weights between 14 and 35 kDa (data not shown).

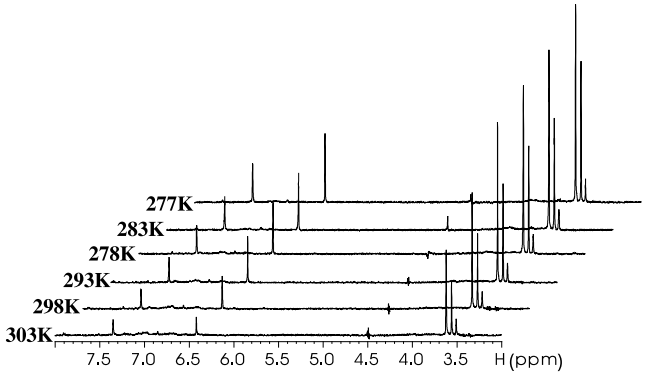

Fig. 5. STD spectra of 4.0 mM TMP with 120 μM DHFR at different temperatures. The spectra are scaled in their references (peak intensities of all references are overlapped). Data were collected on a 500 MHz spectrometer. The protein was irradiated with a Gaussian shaped pulse train at 0.9 ppm for 2.0 s with a total recovery delay of 3.0 s. A CPMG T2 filter of 32.9 ms was used. Temperature was controlled by a Bruker BVT 3000.

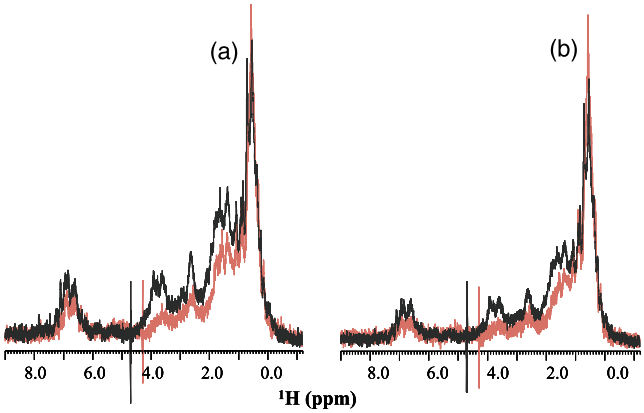

Fig. 6. (a) STD spectra of 100 μM DHFR at 277 K (black) and 303 K (red) recorded with a saturation time of 2.0 s. (b) STD spectra of 100 μM DHFR at 277 K (black) and 303 K (red) recorded with a saturation time of 0.5 s. The spectra are shown in the scale of equal reference intensity. All data were acquired on a 500 MHz spectrometer. The protein was irradiated with a Gaussian shaped pulse train and the total recovery time was set to 3.0 s. Temperature was controlled by a Bruker BVT 3000.

4. Conclusion

During the presaturation period, saturation diffuses over the entire protein and transfers progressively from the target to the ligand. However, all magnetizations, including the transferred saturation, decay because of relaxation. The relaxation mechanism during the saturation period is related not only to the observed ligand but also to the saturated protein. Several other mechanisms, such as spin diffusion within the target, magnetization transferring from the target to the ligand, and spin diffusion between the ligand protons, also occur during saturation. A theoretical model of complete relaxation and conformation exchange matrix was used to study other effects on STD intensity [41]. Relaxation is one of the major components in the complete matrix, but only an estimated relaxation rate for nonspecific relaxation was used to build the relaxation matrix. Measurement or estimation of the relaxation effect on STD has not been exploited in order to achieve the real rate of intermolecular cross-relaxation.

We have noticed in our work that aromatic protons generally give rise to stronger STD than aliphatic protons. Our results indicate that the T1 of the ligand proton has severe interference in the STD measurement. This effect is not critical for determining the extent of binding for screening but is important for the binding epitope to characterize the target–ligand interactions. STD experiments may not give the appropriate epitope map if the T1 of individual ligand protons are significantly different. When a typical saturation time is used, 2 s in this case, the STD epitope map will be ordered by relaxation time T1. We believe that STD is a fast, easy method for screening the binding components from a mixture and is still a good choice for determining the epitope map if the individual T1 relaxation times are similar. But great care should be taken when STD is employed to create an epitope map for binding. Correct information in an epitope map is important to direct structure–activity relationship (SAR) work of a potential compound on the target. If the T1 of individual protons are not similar, relatively short saturation times should be applied or other methods, such as trNOE [7] or diffusion NMR [12], should be used.

The efficiency of ligand saturation largely depends on several factors, such as the disassociation rate constant, concentration ratio of ligand and target, saturation duration, irradiation offset and protein properties (like molecular tumbling rate). As described above, the choice of irradiation offset is limited by the dispersion of ligand signals. The irradiation at protein methyls was found to yield the most efficient saturation. Adjusting the length and amplitude of shaped pulse can also be used to modify the saturation offset. T1 relaxation affects the set of saturation time for binding epitope. Lowering temperature was proved to improve STD measurements of ligands with small to medium size targets.

Acknowledgment

The authors thank Dr. Cynthia K. Larive for useful discussions.

References

[1] S.B. Shuker, P.J. Hajduk, R.P. Meadows, S.W. Fesik, Discovering high-affinity ligands for proteins: SAR by NMR, Science 274 (1996) 1531–1534.
[2] P.J. Hajduk, D.J. Augeri, J. Mack, R. Mendoza, J. Yang, S.F. Betz, S.W. Feisk, NMR-based screening of proteins containing ^{13}C-labeled methyl groups, J. Am. Chem. Soc. 122 (2000) 7898–7904.
[3] P.J. Hajduk, M. Bures, J. Praestgaard, S.W. Fesik, Privileged molecules for protein binding identified from NMR-based screening, J. Med. Chem. 43 (2000) 3443–3447.
[4] F. Ni, Recent developments in transferred NOE methods, Prog. Nucl. Magn. Reson. 26 (1994) 517–606.
[5] T. Peters, Transfer NOE experiments for the study of carbohydrate–protein interactions, Carbohydr. Chem. Biol. 2 (2000) 1003–1023.
[6] M.J.J. Blommers, W. Stark, C.E. Jones, D. Head, C.E. Owen, W. Jahnke, Transferred cross-correlated relaxation complements transferred NOE: structure of an IL-4R-derived peptide bound to STAT-6, J. Am. Chem. Soc. 121 (1999) 1949–1953.
[7] M. Mayer, B. Meyer, Mapping the active site of angiotensin-converting enzyme by transferred NOE spectroscopy, J. Med. Chem. 43 (2000) 2093–2099.
[8] L. Herfurth, T. Weimar, T. Peters, Application of 3D-TOCSY-trNOESY for the assignment of bioactive ligands from mixtures, Angew. Chem. Int. Ed. Eng. 39 (2000) 2097–2099.
[9] D. Li, E.F. DeRose, R.E. London, The inter-ligand Overhauser effect: a powerful new NMR approach for mapping structural relationships of macromolecular ligands, J. Biol. NMR 15 (1999) 71–76.
[10] D. Li, L.A. Levy, S.A. Gabel, M.S. Lebetkin, E.F. DeRose, M.J. Wall, E.E. Howell, R.E. London, Interligand overhauser effects in Type II dihydrofolate reductase, Biochemistry 40 (2001) 4242–4252.
[11] R.E. London, Theoretical analysis of the inter-ligand overhauser effect: a new approach for mapping structural relationships of macromolecular ligands, J. Magn. Reson. 141 (1999) 301–311.
[12] J. Yan, A.D. Kline, H. Mo, E.R. Zartler, M.J. Shapiro, Epitope mapping of ligand–receptor interactions by diffusion NMR, J. Am. Chem. Soc. 124 (2002) 9984–9985.
[13] M. Lin, M.J. Shapiro, Mixture analysis in combinatorial chemistry. Application of diffusion-resolved NMR spectroscopy, J. Org. Chem. 61 (1996) 7617–7619.
[14] M. Lin, M.J. Shapiro, J.R. Wareing, Diffusion-edited NMR-affinity NMR for direct observation of molecular interactions, J. Am. Chem. Soc. 119 (1997) 5249–5250.
[15] P.J. Hajduk, E.T. Olejniczak, S.W. Fesik, One-dimensional relaxation- and diffusion-edited NMR methods for screening compounds that bind to macromolecules, J. Am. Chem. Soc. 119 (50) (1997) 12257–12261.
[16] R.C. Anderson, M. Lin, M.J. Shapiro, Affinity NMR: decoding DNA binding, J. Comb. Chem. 1 (1999) 69–72.
[17] S.R. LaPlante, N. Aubry, R. Deziel, F. Ni, P. Xu, Transferred ^{13}C T1 relaxation at natural isotopic abundance: a practical method

for determining site-specific changes in ligand flexibility upon binding to a macromolecule, J. Am. Chem. Soc. 120 (2000) 12530–12535.
[18] A. Chen, M.J. Shapiro, NOE pumping: a novel NMR technique for identification of compounds with binding affinity to macromolecules, J. Am. Chem. Soc. 120 (1998) 10258–10259.
[19] A. Chen, M.J. Shapiro, NOE pumping. 2. A high-throughput method to determine compounds with binding affinity to macromolecules by NMR, J. Am. Chem. Soc. 122 (2000) 414.
[20] W. Jahnke, P. Floersheim, C. Ostermeier, X. Zhang, R. Hemmig, K. Hurth, D.P. Uzunov, NMR reporter screening for the detection of high-affinity ligands, Angew. Chem. Int. Ed. 41 (2002) 3420–3423.
[21] A.H. Siriwardena, F. Tian, S. Noble, J.H. Prestegard, A straightforward NMR-spectroscopy-based method for rapid library screening, Angew. Chem. Int. Ed. 41 (2002) 3454–3457.
[22] C. Dalvit, P. Pevarello, M. Tato, M. Veronesi, A. Vulpetti, M. Sundstrom, Identification of compounds with binding affinity to proteins via magnetization transfer from bulk water, J. Biol. NMR 18 (2000) 65–68.
[23] C. Dalvit, M. Fasolini, M. Flocco, S. Knapp, P. Pevarello, M. Veronesi, NMR-based screening with competition water-ligand observed via gradient spectroscopy experiments: detection of high-affinity ligands, J. Med. Chem. 45 (2002) 2610–2614.
[24] R. Meinecke, B. Meyer, Determination of the binding specificity of an integral membrane protein by saturation transfer difference NMR: RGD peptide ligands binding to integrin αIIbβ3, J. Med. Chem. 44 (2001) 3059–3065.
[25] M. Mayer, B. Meyer, Characterization of ligand binding by saturation transfer difference NMR spectroscopy, Angew. Chem. Int. Ed. Eng. 38 (1999) 1784–1788.
[26] J. Klein, R. Meinecke, M. Mayer, B. Meyer, Detecting binding affinity to immobilized receptor proteins in compound libraries by HR-MAS-STD NMR, J. Am. Chem. Soc. 121 (1999) 5336–5337.
[27] M. Mayer, B. Meyer, Group epitope mapping by saturation transfer difference NMR to identify segments of a ligand in direct contact with a protein receptor, J. Am. Chem. Soc. 123 (2001) 6108–6117.
[28] M. Vogtherr, T. Peters, Application of NMR based binding assays to identify key hydroxy groups for intermolecular recognition, J. Am. Chem. Soc. 122 (2000) 6093–6099.
[29] H. Moller, N. Serttas, H. Paulsen, J.M. Burchell, J. Taylor-Papadimitriou, B. Meyer, NMR-based determination of the binding epitope and conformational analysis of MUC-1 glycopeptides and peptides bound to the breast cancer-selective monoclonal antibody SM3, Eur. J. Biochem. 269 (2002) 1444–1455.
[30] J. Feeney, NMR studies of ligand binding to dihydrofolate reductase, Angew. Chem. Int. Ed. 39 (2000) 291–312.
[31] G. Martorell, M.J. Gradwell, B. Birdsall, C.J. Bauer, T.A. Frenkiel, H.T.A. Cheung, V.I. Polshakov, L. Kuyper, J. Feeney, Solution structure of bound trimethoprim in its complex with *Lactobacillus casei* dihydrofolate reductase, Biochemistry 33 (1994) 12416–12426.
[32] V.I. Polshakov, B. Birdsall, J. Feeney, Characterization of rates of ring-flipping in trimethoprim in its ternary complexes with *Lactobacillus casei* dihydrofolate reductase and coenzyme analogues, Biochemistry 38 (1999) 15962–15969.
[33] R. Li, R. Sirawaraporn, P. Chitnumsub, W. Sirawaraporn, J. Wooden, F. Athappilly, S. Turley, W.G. Hol, Three-dimensional structure of *M. tuberculosis* dihydrofolate reductase reveals opportunities for the design of novel tuberculosis drugs, J. Mol. Biol. 295 (2000) 307.
[34] D.A. Matthews, J.T. Bolin, J.M. Burridge, D.J. Filman, K.W. Volz, B.T. Kaufman, C.R. Beddell, J.N. Champness, D.K. Stammers, J. Kraut, Refined crystal structures of *Escherichia coli* and chicken liver dihydrofolate reductase containing bound trimethoprim, J. Biol. Chem. 260 (1985) 381–391.
[35] L.F. Kuyper, B. Roth, D.P. Baccanari, R. Ferone, C.R. Beddell, J.N. Champness, D.K. Stammers, J.G. Dann, F.E.A. Norrington, Receptor-based design of dihydrofolate reductase inhibitors: comparison of crystallographically determined enzyme binding with enzyme affinity in a series of carboxy-substituted trimethoprim analogs, J. Med. Chem. 25 (1982) 1120–1122.
[36] W.D. Morgan, B. Birdsall, V.I. Polshakov, D. Sali, I. Kompis, J. Feeney, Solution structure of a brodimoprim analogue in its complex with *Lactobacillus casei* dihydrofolate reductase, Biochemistry 34 (1995) 11690.
[37] H.Y. Carr, E.M. Purcell, Effects of diffusion on free precession in nuclear magnetic resonance experiments, Phys. Rev. 94 (1954) 630–638.
[38] S. Meiboom, D. Gill, Modified spin-echo method for measuring nuclear relaxation times, Rev. Sci. Instr. 29 (1958) 688–691.
[39] M. Liu, X.-A. Mao, C. Ye, H. Huang, J.K. Nicholson, J.C. Lindon, Improved WATERGATE pulse sequences for solvent suppression in NMR spectroscopy, J. Mag. Res. 132 (1998) 125–129.
[40] G.C.K. Roberts, J. Feeney, A.S.V. Burgen, S. Daluge, The charge state of trimethoprim bound to *Lactobacillus casei* dihydrofolate reductase, FEBS Lett. 131 (1981) 85–88.
[41] V. Jayalakshim, N.R. Krishna, Complete relaxation and conformational exchange matrix (CORCEMA) analysis of intermolecular saturation transfer effects in reversibly forming ligand-receptor complexes, J. Magn. Reson. 155 (2002) 106–118.